

Mastering Atari Games with Limited Data

Weirui Ye* Shaohuai Liu* Thanard Kurutach† Pieter Abbeel† Yang Gao*‡

*Tsinghua University, †UC Berkeley, ‡ Shanghai Qi Zhi Institute

Abstract

Reinforcement learning has achieved great success in many applications. However, sample efficiency remains a key challenge, with prominent methods requiring millions (or even billions) of environment steps to train. Recently, there has been significant progress in sample efficient image-based RL algorithms; however, consistent human-level performance on the Atari game benchmark remains an elusive goal. We propose a sample efficient model-based visual RL algorithm built on MuZero, which we name EfficientZero. Our method achieves 190.4% mean human performance and 116.0% median performance on the Atari 100k benchmark with only two hours of real-time game experience and outperforms the state SAC in some tasks on the DMControl 100k benchmark. This is the first time an algorithm achieves super-human performance on Atari games with such little data. EfficientZero’s performance is also close to DQN’s performance at 200 million frames while we consume 500 times less data. EfficientZero’s low sample complexity and high performance can bring RL closer to real-world applicability. We implement our algorithm in an easy-to-understand manner and it is available at <https://github.com/YeWR/EfficientZero>. We hope it will accelerate the research of MCTS-based RL algorithms in the wider community.

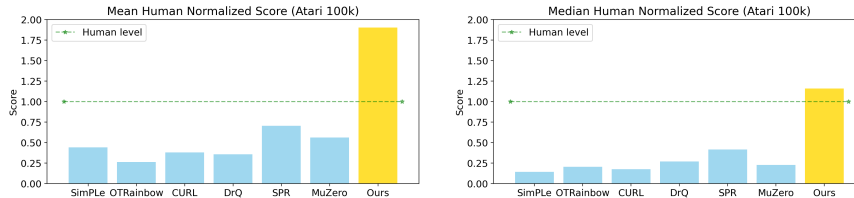


Figure 1: Our proposed method EfficientZero is 170% and 180% better than the previous SoTA performance in mean and median human normalized score and is the first to outperform the average human performance on the Atari 100k benchmark. The high sample efficiency and performance of EfficientZero can bring RL closer to the real-world applications.

1 Introduction

Reinforcement learning has achieved great success on many challenging problems. Notable work includes DQN [26], AlphaGo [37] and OpenAI Five [6]. However, most of these works come at the cost of a large number of environmental interactions. For example, AlphaZero [38] needs to play 21 million games at training time. On the contrary, a professional human player can only play around 5 games per day, meaning it would take a human player 11,500 years to achieve the same amount of experience. The sample complexity might be less of an issue when applying RL algorithms in simulation and games. However, when it comes to real-world problems, such as robotic

*{ywr20, liush20}@mails.tsinghua.edu.cn, gaoyangiiis@tsinghua.edu.cn

†{thanard.kurutach, pabbeel}@berkeley.edu

manipulation, healthcare, and advertisement recommendation systems, achieving high performance while maintaining low sample complexity is the key to viability.

People have made a lot of progress in sample efficient RL in the past years [9, 11, 39, 24, 22, 36, 19]. Among them, model-based methods have attracted a lot of attention, since both the data from real environments and the “imagined data” from the model can be used to train the policy, making these methods particularly sample-efficient [9, 11]. However, most of the successes are in state-based environments. In image-based environments, some model-based methods such as MuZero [31] and Dreamer V2 [15] achieve super-human performance, but they are not sample efficient; other methods such as SimPLe [19] is quite efficient but achieve inferior performance (0.144 human normalized median scores). Recently, data-augmented and self-supervised methods applied to model-free methods have achieved more success in the data-efficient regime [36]. However, they still fail to achieve the levels which can be expected of a human.

Therefore, for improving the sample efficiency as well as keeping superior performance, we find the following three components are essential to the model-based visual RL agent: a self-supervised environment model, a mechanism to alleviate the model compounding error, and a method to correct the off-policy issue. In this work, we propose EfficientZero, a model-based RL algorithm that achieves high performance with limited data. Our proposed method is built on MuZero. We make three critical changes: (1) use self-supervised learning to learn a temporally consistent environment model, (2) learn the *value prefix* in an end-to-end manner, thus helping to alleviate the compounding error in the model, (3) use the learned model to correct off-policy value targets.

As illustrated as Figure 1, our model achieves state-of-the-art performance on the widely used Atari [5] 100k benchmark and it achieves super-human performance with only 2 hours of real-time gameplay. More specifically, our model achieves 190.4% mean human normalized performance and 116.0% median human normalized performance. As a reference, DQN [26] achieves 220% mean human normalized performance, and 96% median human normalized performance, at the cost of 500 times more data (200 million frames). To further verify the effectiveness of EfficientZero, we conduct experiments on some simulated robotics environments of the DeepMind Control (DMControl) suite. It achieves state-of-the-art performance and outperforms the state SAC which directly learns from the ground truth states. Our sample efficient and high-performance algorithm opens the possibility of having more impact on many real-world problems.

2 Related Work

2.1 Sample Efficient Reinforcement Learning

Sample efficiency has attracted significant work in the past. In RL with image inputs, model-based approaches [14, 13] which model the world with both a stochastic and a deterministic component, have achieved promising results for simulated robotic control. Kaiser et al. [19] propose to use an action-conditioned video prediction model, along with a policy learning algorithm. It achieves the first strong performance on Atari games with as little as 400k frames. However, Kielak [20] and van Hasselt et al. [44] argue that this is not necessary to achieve strong results with model-based methods, and they show that when tuned appropriately, Rainbow [17] can achieve comparable results.

Recent advances in self-supervised learning, such as SimCLR [7], MoCo [16], SimSiam [8] and BYOL [12] have inspired representation learning in image-based RL. Srinivas et al. [39] propose to use contrastive learning in RL algorithms and their work achieves strong performance on image-based continuous and discrete control tasks. Later, Laskin et al. [24] and Kostrikov et al. [22] find that contrastive learning is not necessary, but with data augmentations alone, they can achieve better performance. Schwarzer et al. [36] propose a temporal consistency loss, which is combined with data augmentations and achieves state-of-the-art performance. Notably, our self-supervised consistency loss is quite similar to Schwarzer et al. [36], except we use SimSiam [7] while they use BYOL [12] as the base self-supervised learning framework. However, Schwarzer et al. [36] only apply the learned representations in a model-free manner, while we combine the learned model with model-based exploration and policy improvement, thus leading to more efficient use of the environment model.

Despite the recent progress in the sample-efficient RL, today’s RL algorithms are still well behind human performance when the amount of data is limited. Although traditional model-based RL is considered more sample efficient than model-free ones, current model-free methods dominate in

terms of performance for image-input settings. In this paper, we propose a model-based RL algorithm that for the first time, achieves super-human performance on Atari games with limited data.

2.2 Reinforcement Learning with MCTS

Temporal difference learning [26, 43, 45, 17] and policy gradient based methods [27, 25, 33, 35] are two types of popular reinforcement learning algorithms. Recently, Silver et al. [37] propose to use MCTS as a policy improvement operator and has achieved great success in many board games, such as Go, Chess, and Shogi [38]. Later, the algorithm is adapted to learn the world model at the same time [31]. It has also been extended to deal with continuous action spaces [18] and offline data [32]. These MCTS RL algorithms are a hybrid of model-based learning and model-free learning.

However, most of them are trained with a lot of environmental samples. Our method is built on top of MuZero [31], and we demonstrate that our method can achieve higher sample efficiency while still achieving competitive performance on the Atari 100k benchmark. de Vries et al. [10] have studied the potential of using auxiliary loss similar to our self-supervised consistency loss. However, they only test on two low dimensional state-based environments and find the auxiliary loss has mixed effects on the performance. On the contrary, we find that the consistency loss is critical in most environments with high dimensional observations and limited data.

2.3 Multi-Step Value Estimation

In Q-learning [46], the target Q value is computed by one step backup. In practice, people find that incorporating multiple steps of rewards at once, i.e. $z_t = \sum_{i=0}^{k-1} \gamma^i u_{t+i} + \gamma^k v_{t+k}$, where u_{t+i} is the reward from the replay buffer, v_{t+k} is the value estimation from the target network, to compute the value target z_t leads to faster convergence [26, 17]. However, the use of multi-step value has off-policy issues, since u_{t+i} are not generated by the current policy. In practice, this issue is usually ignored when there is a large amount of data since the data can be thought as approximately on-policy. TD(λ) [40] and GAE [34] improve the value estimation by better trading off the bias and the variance, but they do not deal with the off-policy issue. Recently, image input model-based algorithms such as Kaiser et al. [19] and Hafner et al. [13] use model imaginary rollouts to avoid the off-policy issue. However, this approach has the risk of model exploitation. Asadi et al. [2] proposed a multi-step model to combat the compounding error. Our proposed model-based off-policy correction method starts from the rewards in the real-world experience and uses model-based value estimate to bootstrap. Our approach balances between the off-policy issue and model exploitation.

3 Background

3.1 MuZero

Our method is built on top of the MuZero Reanalyze [31] algorithm. For brevity, we refer to it as MuZero throughout the paper. MuZero is a policy learning method based on the Monte-Carlo Tree Search (MCTS) algorithm. The MCTS algorithm operates with an environment model, a prior policy function, and a value function. The environment model is represented as the reward function \mathcal{R} and the dynamic function \mathcal{G} : $r_t = \mathcal{R}(s_t, a_t)$, $\hat{s}_{t+1} = \mathcal{G}(s_t, a_t)$, which are needed when MCTS expands a new node. In MuZero, the environment model is learned. Thus the reward and the next state are approximated. Besides, the predicted policy p_t acts as a search prior over actions of a node. It helps the MCTS focus on more promising actions when expanding the node. MCTS also needs a value function $\mathcal{V}(s_t)$ that measures the expected return of the node s_t , which provides a long-term evaluation of the tree’s leaf node without further search. MCTS will output an action visit distribution π_t over the root node, which is potentially a better policy, compared to the current neural network. Thus, the MCTS algorithm can be thought of as a policy improvement operator.

In practice, the environment model, policy function, and value function operate on a hidden abstract state s_t , both for computational efficiency and ease of environment modeling. The abstract state is extracted by a representation function \mathcal{H} on observations o_t : $s_t = \mathcal{H}(o_t)$. All of the mentioned models above are usually represented as neural networks. During training, the algorithm collects roll-out data in the environment using MCTS, resulting in potentially higher quality data than the current neural network policy. The data is stored in a replay buffer. The optimizer minimizes the

following loss on the data sampled from the replay buffer:

$$\mathcal{L}(u_t, r_t) + \lambda_1 \mathcal{L}(\pi_t, p_t) + \lambda_2 \mathcal{L}(z_t, v_t) \quad (1)$$

Here, u_t is the reward from the environment, $r_t = \mathcal{R}(s_t, a_t)$ is the predicted reward, π_t is the output visit count distribution of the MCTS, $p_t = \mathcal{P}(s_t)$ is the predicted policy, $z_t = \sum_{i=0}^{k-1} \gamma^i u_{t+i} + \gamma^k v_{t+k}$ is the bootstrapped value target and $v_t = \mathcal{V}(s_t)$ is the predicted value. Specifically, the reward function \mathcal{R} , policy function \mathcal{P} , value function \mathcal{V} , the representation function \mathcal{H} and the dynamics function \mathcal{G} are trainable neural networks. It is worth noting that MuZero does not explicitly learn the environment model. Instead, it solely relies on the reward, value, and policy prediction to learn the model.

3.2 Monte-Carlo Tree Search

Monte-Carlo Tree Search [1, 37, 38, 15], or MCTS, is a heuristic search algorithm. In our setup, MCTS is used to find an action policy that is better than the current neural network policy.

More specifically, MCTS needs an environment model, including the reward function and the next-state function. It also needs a value function and a policy function, which act as heuristics for the tree search. MCTS operates by expanding a search tree from the current node. It saves computation by selectively expanding a few nodes. In order to find a high-quality decision, the tree expansion process has to balance between exploration versus exploitation, i.e. balance between expanding a node that is promising with many visits versus expanding a node with lower performance but fewer visits. MCTS employs the UCT [29, 21] rule, i.e. UCB [3] on trees. At every node expansion step, UCT will select a node as follows [15]:

$$a^k = \arg \max_a \left\{ Q(s, a) + P(s, a) \frac{\sqrt{\sum_b N(s, b)}}{1 + N(s, a)} \left(c_1 + \log \left(\frac{\sum_b N(s, b) + c_2 + 1}{c_2} \right) \right) \right\} \quad (2)$$

where, $Q(s, a)$ is the current estimate of the Q-value, $P(s, a)$ is the current neural network policy for selecting this action, helping the MCTS prioritize exploring promising part of the tree. During training time, $P(s, a)$ is usually perturbed by noises to allow explorations. $N(s, a)$ denotes how many times this state-action pair is visited in the tree search, and $N(s, b)$ denote that of a 's siblings. Thus this term will encourage the search to visit the nodes whose siblings are visited often, but itself less visited. Finally, the last term gives a weights to the previous terms.

After expanding the nodes for a pre-defined number of times, the MCTS will return how many times each action under the root node is visited, as the improved policy to the root node. Thus, MCTS can be considered as a policy improvement operator in the RL setting.

4 EfficientZero

Model-based algorithms have achieved great success in sample-efficient learning from low-dimensional states. However, current visual model-based algorithms either require large amounts of training data or exhibit inferior performance to model-free algorithms in data-limited settings [36]. Many previous works even suspect whether model-based algorithms can really offer data efficiency when using image observations [44]. We provide a positive answer here. We propose the EfficientZero, a model-based algorithm built on the MCTS, that achieves super-human performance on the 100k Atari benchmark, outperforming the previous SoTA to a large degree.

When directly running MCTS-based RL algorithms such as MuZero, we find that they do not perform well on the limited-data benchmark. Through our ablations, we confirm the following three issues which pose challenges to algorithms like MuZero in data-limited settings.

Lack of supervision on environment model. First, the learned model in the environment dynamics is only trained through the reward, value and policy functions. However, the reward is only a scalar signal and in many scenarios, the reward will be sparse. Value functions are trained with bootstrapping, and thus are noisy. Policy functions are trained with the search process. None of the reward, value and policy losses can provide enough training signals to learn the environment model.

Hardness to deal with aleatoric uncertainty. Second, we find that even with enough data, the predicted rewards still have large prediction errors. This is caused by the aleatoric uncertainty of the underlying environment. For example, the environment is hard to model. The reward prediction

errors will accumulate when expanding the MCTS tree to a large depth, resulting in sub-optimal performance in exploration and evaluation.

Off-policy issues of multi-step value. Lastly, when computing the value target, MuZero uses the multi-step reward observed in the environment. Although this allows the reward to be propagated to the value function faster, we find that it suffers from severe off-policy issues and hinders convergence in the limited data scenario.

To address the above issues, we propose the following three critical modifications, which can greatly improve performance when samples are limited.

4.1 Self-Supervised Consistency Loss

In previous MCTS RL algorithms, the environment model is either given or only trained with rewards, values, and policies, which cannot provide sufficient training signals due to their scalar nature. The problem is more severe when the reward is sparse or the bootstrapped value is not accurate. The MCTS policy improvement operator heavily relies on the environment model. Thus, it is vital to have an accurate one.

We notice that the output \hat{s}_{t+1} from the dynamic function \mathcal{G} should be the same as s_{t+1} , i.e. the output of the representation function \mathcal{H} with input of the next observation o_{t+1} (Fig. 2). This can help to supervise the predicted next state \hat{s}_{t+1} using the actual s_{t+1} , which is a tensor with at least a few hundred dimensions. This provides \hat{s}_{t+1} with much more training signals than the default scalar reward and value.

More specifically, we adopt the recently proposed SimSiam [8] self-supervised framework. SimSiam [8] is a self-supervised method that takes two augmentation views of the same image and pulls the output of the second branch close to that of the first branch, where the first branch is an encoder network without gradient, and the second branch is the same encoder network with the gradient and a predictor head. The predictor head can simply be a two-layer MLP.

Note that SimSiam only learns the representation of individual images, and is not aware of how different images are connected. The learned image representations of SimSiam might not be a good candidate for learning the environment transition function, since adjacent observations might be encoded to very different representation encodings. We propose a self-supervised method that learns the transition function, along with the image representation function in an end-to-end manner. Figure 2 shows our method. Since we aim to learn the transition between adjacent observations, we pull o_t and o_{t+1} close to each other. The transition function is applied after the representation of o_t , such that s_t is transformed to \hat{s}_{t+1} , which now represents the same entity as the other branch. Then both of s_{t+1} and \hat{s}_{t+1} go through a common projector network. Since s_{t+1} is potentially a more accurate description of o_{t+1} compared to \hat{s}_{t+1} , we make the o_{t+1} branch as the target branch. It is common in self-supervised learning that the second or the third layer from the last is chosen as the features for some reason. Here, we choose the outputs from the representation network or the dynamics network as the hidden states rather than those from the projector or the predictor.

The two adjacent observations provide two views of the same entity. In practice, we find that applying augmentations to observations such as a random small shift of 0-4 pixels on the image helps to further improve the learned representation quality [39, 36]. We also unroll the dynamic function recurrently for 5 further steps and also pull \hat{s}_{t+k} close to s_{t+k} ($k = 1, \dots, 5$). Please see App. A.1 for more implementation details.

4.2 End-To-End Prediction of the Value Prefix

In model-based learning, the agent needs to predict the future states conditioned on the current state and a series of hypothetical actions. The longer the prediction, the harder to predict it accurately, due

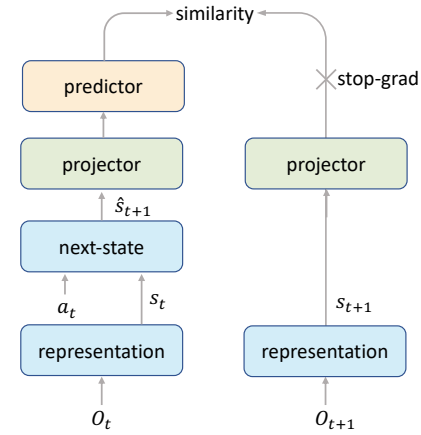


Figure 2: The self-supervised consistency loss.

to the compounding error in the recurrent rollouts. This is called the state aliasing problem. The environment model plays an important role in MCTS. The state aliasing problem harms the MCTS expansion, which will result in sub-optimal exploration as well as sub-optimal action search.

Predicting the reward from an aliased state is a hard problem. For example, as shown in Figure 3, the right agent loses the ball. If we only see the first observation, along with future actions, it is very hard both for an agent and a human to predict at which exact future timestep the player would lose a point. However, it is easy to predict the agent will miss the ball after a sufficient number of timesteps if he does not move. In practice, a human will never try to predict the exact step that he loses the point but will imagine over a longer horizon and thus get a more confident prediction.

Inspired by this intuition, we propose an end-to-end method to predict the *value prefix*. We notice that the predicted reward is always used in the estimation of the Q-value $Q(s, a)$ in UCT of Equation 2

$$Q(s_t, a) = \sum_{i=0}^{k-1} \gamma^i r_{t+i} + \gamma^k v_{t+k} \quad (3)$$

, where r_{t+i} is the reward predicted from unrolled state \hat{s}_{t+i} . We name the sum of rewards $\sum_{i=0}^{k-1} \gamma^i r_{t+i}$ as the value prefix, since it is used as a prefix in the later Q-value computation.

We propose to predict value prefix from the unrolled states $(s_t, \hat{s}_{t+1}, \dots, \hat{s}_{t+k-1})$ in an end-to-end manner, i.e. value-prefix = $f(s_t, \hat{s}_{t+1}, \dots, \hat{s}_{t+k-1})$. Here f is some neural network architecture that takes in a variable number of inputs and outputs a scalar. We choose the LSTM in our experiment. During the training time, the LSTM is supervised at every time step, since the value prefix can be computed whenever a new state comes in. This per-step rich supervision allows the LSTM can be trained well even with limited data. Compared with the naive per step reward prediction and summation approach, the end-to-end value prefix prediction is more accurate, because it can automatically handle the intermediate state aliasing problem. See Experiment Section 5.3 for empirical evaluations. As a result, it helps the MCTS to explore better, and thus increases the performance. See App.A.1 for architectural details.

4.3 Model-Based Off-Policy Correction

In MCTS RL algorithms, the value function fits the value of the current neural network policy. However, in practice as MuZero Reanalyze does, the value target is computed by sampling a trajectory from the replay buffer and computing: $z_t = \sum_{i=0}^{k-1} \gamma^i u_{t+i} + \gamma^k v_{t+k}$. This value target suffers from off-policy issues, since the trajectory is rolled out using an older policy, and thus the value target is no longer accurate. When data is limited, we have to reuse the data sampled from a much older policy, thus exaggerating the inaccurate value target issue.

In previous model-free settings, there is no straightforward approach to fix this issue. On the contrary, since we have a model of the environment, we can use the model to imagine an "online experience". More specifically, we propose to use rewards of a dynamic horizon l from the old trajectory, where $l < k$ and l should be smaller if the trajectory is older. This reduces the policy divergence by fewer rollout steps. Further, we redo an MCTS search with the current policy on the last state s_{t+l} and compute the empirical mean value at the root node. This effectively corrects the off policy issue using imagined rollouts with current policy and reduces the increased bias caused by setting l less than k . Formally, we propose to use the following value target:

$$z_t = \sum_{i=0}^{l-1} \gamma^i u_{t+i} + \gamma^l \nu_{t+l}^{\text{MCTS}} \quad (4)$$

where $l \leq k$ and the older the sampled trajectory, the smaller the l . $\nu^{\text{MCTS}}(s_{t+l})$ is the root value of the MCTS tree expanded from s_{t+l} with the current policy, as MuZero non-Reanalyze does. See App.A.4 for how to choose l . In practice, the computation cost of the correction is two times on the reanalyzed side. However, the training will not be affected due to the parallel implementation.

5 Experiments

In this section, we aim to evaluate the sample efficiency of the proposed algorithm. Here, the sample efficiency is measured by the performance of each algorithm at a common, small amount of environment transitions, i.e. the better the performance, the higher the sample efficiency. More specifically, we use the Atari 100k benchmark. Intuitively, this benchmark asks the agent to learn to play Atari games within two hours of real-world game time. Additionally, we conduct some ablation studies to investigate and analyze each component on Atari 100k. To further show the sample efficiency, we apply EfficientZero to some simulated robotics environments on the DMControl 100k benchmark, which contains the same 100k environment steps.

5.1 Environments

Atari 100k Atari 100k was first proposed by the SimPLe [19] method, and is now used by many sample-efficient RL works, such as Srinivas et al. [39], Laskin et al. [24], Kostrikov et al. [22], Schwarzer et al. [36]. The benchmark contains 26 Atari games, and the diverse set of games can effectively measure the performance of different algorithms. The benchmark allows the agent to interact with 100 thousand environment steps, i.e. 400 thousand frames due to a frameskip of 4, with each environment. 100k steps roughly correspond to 2 hours of real-time gameplay, which is far less than the usual RL settings. For example, DQN [26] uses 200 million frames, which is around 925 hours of real-time gameplay. Note that the human player’s performance is tested after allowing the human to get familiar with the game after 2 hours as well. We report the raw performance on each game, as well as the mean and median of the human normalized score. The human normalized score is defined as: $(\text{score}_{\text{agent}} - \text{score}_{\text{random}}) / (\text{score}_{\text{human}} - \text{score}_{\text{random}})$.

We compare our method to the following baselines. (1) SimPLe [19], a model-based RL algorithm that learns an action conditional video prediction model and trains PPO within the learned environment. (2) OTRainbow [20], which tunes the hyper-parameters of the Rainbow [17] method to achieve higher sample efficiency. (3) CURL [39], which uses contrastive learning as a side task to improve the image representation quality. (4) DrQ [22], which adds data augmentations to the input images while learning the original RL objective. (5) SPR [36], the previous SoTA in Atari 100k which proposes to augment the Rainbow [17] agent with data augmentations as well as a multi-step consistency loss using BYOL-style self-supervision. (6) MuZero [31] with our implementations and the same hyper-parameters as EfficientZero. (7) Random Agent (8) Human performance.

DeepMind Control 100k Tassa et al. [41] propose the DMControl suite, which includes some challenging visual robotics tasks with continuous action space. And some works [13, 39] have benchmarked for the sample efficiency on the DMControl 100k which contains 100k environment steps data. Since the MCTS-based methods cannot deal with tasks with continuous action space, we discretize each dimension into 5 discrete slots in MuZero [31] and EfficientZero. To avoid the dimension explosion, we evaluate EfficientZero in three low-dimensional tasks.

We compare our method to the following baselines. (1) Pixel SAC, which applies SAC directly to pixels. (2) SAC-AE [48], which combines the SAC and an auto-encoder to handle image-based inputs. (3) State SAC, which applies SAC directly to ground truth low dimensional states rather than the pixels. (4) Dreamer [13], which learns a world model and is trained in dreamed scenarios. (5) CURL [39], the previous SoTA in DMControl 100k. (6) MuZero [31] with action discretizations.

5.2 Results

Table 1 shows the results of EfficientZero on the Atari 100k benchmark. Normalizing our score with the score of human players, EfficientZero achieves a mean score of 1.904 and a median score of 1.160. As a reference, DQN [26] achieves a mean and median performance of 2.20 and 0.959 on these 26 games. However, it is trained with 500 times more data (200 million frames). For the first time, an agent trained with only 2 hours of game data can outperform the human player in terms of the mean and median performance. Among all games, our method outperforms the human in 14 out of 26 games. Compared with the previous state-of-the-art method (SPR [36]), we are 170% and 180% better in terms of mean and median score respectively.

Apart from the Atari games, EfficientZero achieves remarkable results in the simulated tasks with continuous action space. As shown in Table 2, EfficientZero outperforms CURL, the previous SoTA,

to a considerable degree and keeps a smaller variance but MuZero cannot work well here. Notably, EfficientZero achieves comparable results to the state SAC, which consumes the ground truth states as input and is considered as the oracles.

Table 1: Scores achieved on the Atari 100k benchmark (32 seeds). EfficientZero achieves super-human performance with only 2 hours of real-time game play. Our method is 170% and 180% better than the previous SoTA performance, in mean and median human normalized score respectively.

Game	Random	Human	SimPLe	OTRainbow	CURL	DrQ	SPR	MuZero	Ours
Alien	227.8	7127.7	616.9	824.7	558.2	771.2	801.5	530.0	1140.3
Amidar	5.8	1719.5	88.0	82.8	142.1	102.8	176.3	38.8	101.9
Assault	222.4	742.0	527.2	351.9	600.6	452.4	571.0	500.1	1407.3
Asterix	210.0	8503.3	1128.3	628.5	734.5	603.5	977.8	1734.0	16843.8
Bank Heist	14.2	753.1	34.2	182.1	131.6	168.9	380.9	192.5	361.9
BattleZone	2360.0	37187.5	5184.4	4060.6	14870.0	12954.0	16651.0	7687.5	17938.0
Boxing	0.1	12.1	9.1	2.5	1.2	6.0	35.8	15.1	44.1
Breakout	1.7	30.5	16.4	9.8	4.9	16.1	17.1	48.0	406.5
ChopperCmd	811.0	7387.8	1246.9	1033.3	1058.5	780.3	974.8	1350.0	1794.0
Crazy Climber	10780.5	35829.4	62583.6	21327.8	12146.5	20516.5	42923.6	56937.0	80125.3
Demon Attack	152.1	1971.0	208.1	711.8	817.6	1113.4	545.2	3527.0	13298.0
Freeway	0.0	29.6	20.3	25.0	26.7	9.8	24.4	21.8	21.8
Frostbite	65.2	4334.7	254.7	231.6	1181.3	331.1	1821.5	255.0	313.8
Gopher	257.6	2412.5	771.0	778.0	669.3	636.3	715.2	1256.0	3518.5
Hero	1027.0	30826.4	2656.6	6458.8	6279.3	3736.3	7019.2	3095.0	8530.1
Jamesbond	29.0	302.8	125.3	112.3	471.0	236.0	365.4	87.5	459.4
Kangaroo	52.0	3035.0	323.1	605.4	872.5	940.6	3276.4	62.5	962.0
Krull	1598.0	2665.5	4539.9	3277.9	4229.6	4018.1	3688.9	4890.8	6047.0
Kung Fu Master	258.5	22736.3	17257.2	5722.2	14307.8	9111.0	13192.7	18813.0	31112.5
Ms Pacman	307.3	6951.6	1480.0	941.9	1465.5	960.5	1313.2	1265.6	1387.0
Pong	-20.7	14.6	12.8	1.3	-16.5	-8.5	-5.9	-6.7	20.6
Private Eye	24.9	69571.3	58.3	100.0	218.4	-13.6	124.0	56.3	100.0
Qbert	163.9	13455.0	1288.8	509.3	1042.4	854.4	669.1	3952.0	15458.1
Road Runner	11.5	7845.0	5640.6	2696.7	5661.0	8895.1	14220.5	2500.0	18512.5
Seaquest	68.4	42054.7	683.3	286.9	384.5	301.2	583.1	208.0	1020.5
Up N Down	533.4	11693.2	3350.3	2847.6	2955.2	3180.8	28138.5	2896.9	16095.7
Normed Mean	0.000	1.000	0.443	0.264	0.381	0.357	0.704	0.562	1.904
Normed Median	0.000	1.000	0.144	0.204	0.175	0.268	0.415	0.227	1.160

Table 2: Scores achieved by EfficientZero (mean & standard deviation for 10 seeds) and some baselines on some low-dimensional environments on the DMControl 100k benchmark. EfficientZero achieves state-of-art performance and comparable results to the state-based SAC.

Task	CURL	Dreamer	MuZero	SAC-AE	Pixel SAC	State SAC	EfficientZero
Cartpole, Swingup	582 \pm 146	326 \pm 27	218.5 \pm 122	311 \pm 11	419 \pm 40	835 \pm 22	813\pm 19
Reacher, Easy	538 \pm 233	314 \pm 155	493 \pm 145	274 \pm 14	145 \pm 30	746 \pm 25	952\pm 34
Ball in cup, Catch	769 \pm 43	246 \pm 174	542 \pm 270	391 \pm 82	312 \pm 63	746 \pm 91	942\pm 17

5.3 Ablations

In Section 4, we discuss three issues that prevent MuZero from achieving high performance when data is limited: (1) the lack of environment model supervision, (2) the state aliasing issue, and (3) the off-policy target value issue. We propose three corresponding approaches to fix those issues and demonstrate the usefulness of the combination of those approaches on a wide range of 26 Atari games. In this section, we will analyze each component individually.

Each Component Firstly, we do an ablation study by removing the three components from our full model one at a time. As shown in Table 3, we find that removing any one of the three components will lead to a performance drop compared to our full model. Furthermore, the richer learning signals are the aspect MuZero lacks most in the low-data regime as the largest performance drop is from the version without consistency supervision. As for the performance in the high-data regime, We find that the temporal consistency can significantly accelerate the training. The value prefix seems to be helpful during the early learning process, but not as much in the later stage. The off-policy correction is not necessary as it is specifically designed under limited data.

Table 3: Ablations of the self-supervised consistency, end-to-end value prefix and model-based off-policy correction. We remove one component at a time and evaluate the corresponding version on the 26 Atari games. Each component matters and the consistency one is the most significant. The detailed results are attached in App.A.2 .

Game	Full	w.o. consistency	w.o. value prefix	w.o. off-policy correction
Normed Mean	1.904	0.881	1.482	1.475
Normed Median	1.160	0.340	0.552	0.836

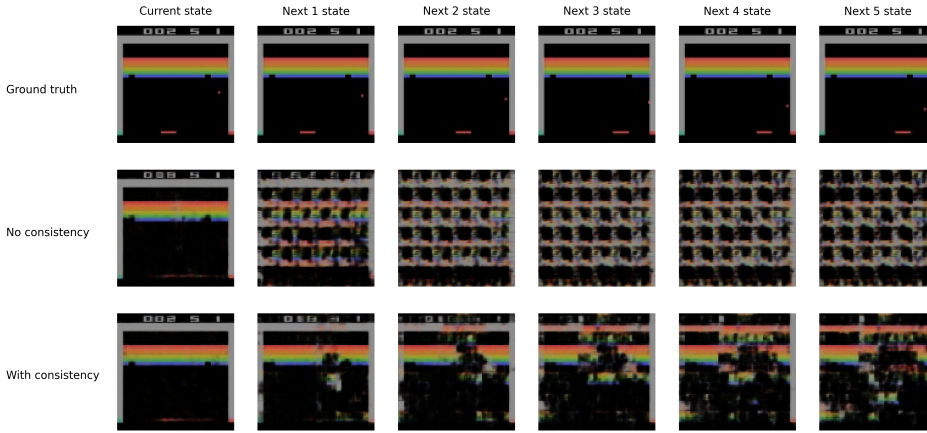


Figure 4: Evaluations of image reconstructions based on latent states extracted from the model with or without self-supervised consistency. The predicted next states with consistency can basically be reconstructed into observations while the ones without consistency cannot.

Temporal Consistency As the version without self-supervised consistency cannot work well in most of the games, we attempt to dig into the reason for such phenomenon. We design a decoder \mathcal{D} to reconstruct the original observations, taking the latent states as inputs. Specifically, the architecture of \mathcal{D} and the \mathcal{H} are symmetrical, which means that all the convolutional layers are replaced by deconvolutional layers in \mathcal{D} and the order of the layers are reversed in \mathcal{D} . Therefore, \mathcal{H} is an encoder to obtain state s_t from observation o_t and \mathcal{D} tries to decode the o_t from s_t . In this ablation, we freeze all parameters of the trained EfficientZero network with or without consistency respectively and the reconstructed results are shown in different columns of Figure 4. We regard the decoder as a tool to visualize the current states and unrolled states, shown in different rows of Figure 4. Here we note that \mathcal{M}_{con} is the trained EfficientZero model with consistency and \mathcal{M}_{non} is the one without consistency.

As shown in Figure 4, in terms of the current state s_t , the observation is reconstructed well enough in the two versions. However, it is remarkable that the the decoder given \mathcal{M}_{non} can not reconstruct images from the unrolled predicted states \hat{s}_{t+k} while the one given \mathcal{M}_{con} can reconstruct the basic observations.

To sum up, there are some distributional shifts between the latent states from the representation network and the states from the dynamics function without consistency. The consistency component can reduce the shift and provide more supervision for training the dynamics network.

Value Prefix We further validate our assumptions in the end-to-end learning of value prefix, i.e. the state aliasing problem will cause difficulty in predicting the reward, and end-to-end learning of value prefix can alleviate this phenomenon.

To fairly compare directly predicting the reward versus end-to-end learning of the value prefix, we need to control for the dataset that both methods are trained on. Since during the RL training, the dataset distribution is determined by the method, we opt to load a half-trained Pong model and rollout total 100k steps as the common static dataset. We split this dataset into a training set and a validation set. Then we run both the direct reward prediction and the value prefix method on the training split.

As shown in Figure 5, we find that the direct reward prediction method has lower losses on the training set. However, the value prefix’s validation error is much smaller when unrolled for 5 steps. This shows that the value prefix method avoids overfitting the hard reward prediction problem, and thus it can reduce the state aliasing problem, reaching a better generalization performance.

Off-Policy Correction

To prove the effectiveness of the off-policy correction component, we compare the error between the target values and the ground truth values with or without off-policy correction. Specifically, the ground truth values are estimated by Monte Carlo sampling.

We train a model for the game UpNDown with total 100k training steps, and collect the trajectories at different training stages respectively (20k, 40k, ..., 100k steps). Then we calculate the ground truth values with the final model. We choose the trajectories at the same stage (20k) and use the final model to evaluate the target values with or without off-policy correction, following the Equation 4. We evaluate the L1 error of the target values and the ground truth, as shown in Table 4. The error of unrolled next 5 states means the average error of the unrolled 1-5 states with dynamics network from current states. The error is smaller in both current states and the unrolled states with off-policy correction. Thus, the correction component does reduce the bias caused by the off-policy issue.

Table 4: Ablations of the off-policy correction: L1 error of the target values versus the ground truth values. Take UpNDown as an example.

States	Current state	Unrolled next 5 states (Avg.)	All states (Avg.)
Value error without correction	0.765	0.636	0.657
Value error with correction	0.533	0.576	0.569

Furthermore, we also ablate the value error of the trajectories at distinct stages in Table 5. We can find that the value error becomes smaller as the trajectories are fresher. This indicates that the off-policy issue is severe due to the staleness of the data. More significantly, the off-policy correction can provide more accurate target value estimation for the trajectories at distinct time-steps as all the errors with correction shown in the table are smaller than those without correction at the same stage.

Table 5: Ablations of the off-policy correction: Average L1 error of the values of the trajectories at distinct stages. Take UpNDown as an example.

Stages of trajectories	20k	40k	60k	80k	100k
Value error without correction	0.657	0.697	0.628	0.574	0.441
Value error with correction	0.569	0.552	0.537	0.488	0.397

6 Discussion

In this paper, we propose a sample-efficient model-based method EfficientZero. It achieves super-human performance on the Atari games with as little as 2 hours of the gameplay experience and state-of-the-art performance on some DMControl tasks. Apart from the full results, we do detailed ablation studies to examine the effectiveness of the proposed components. This work is one step towards running RL in the physical world with complex sensory inputs. In the future, we plan to extend it to more directions, such as a better design for the continuous action space. And we also plan to study the acceleration of MCTS and how to combine this framework with life-long learning.

Figure 5: Training and validation losses of direct reward prediction method and the value prefix method.

Acknowledgments and Disclosure of Funding

This work is supported by the Ministry of Science and Technology of the People’s Republic of China, the 2030 Innovation Megaprojects “Program on New Generation Artificial Intelligence” (Grant No. 2021AAA0150000).

References

- [1] Bruce Abramson. *The expected-outcome model of two-player games*. Morgan Kaufmann, 2014.
- [2] Kavosh Asadi, Dipendra Misra, Seungchan Kim, and Michel L Littman. Combating the compounding-error problem with a multi-step model. *arXiv preprint arXiv:1905.13320*, 2019.
- [3] Peter Auer, Nicolo Cesa-Bianchi, and Paul Fischer. Finite-time analysis of the multiarmed bandit problem. *Machine learning*, 47(2):235–256, 2002.
- [4] Andrew G Barto, Richard S Sutton, and Charles W Anderson. Neuronlike adaptive elements that can solve difficult learning control problems. *IEEE transactions on systems, man, and cybernetics*, (5):834–846, 1983.
- [5] Marc G Bellemare, Yavar Naddaf, Joel Veness, and Michael Bowling. The arcade learning environment: An evaluation platform for general agents. *Journal of Artificial Intelligence Research*, 47:253–279, 2013.
- [6] Christopher Berner, Greg Brockman, Brooke Chan, Vicki Cheung, Przemysław Dębiak, Christy Dennison, David Farhi, Quirin Fischer, Shariq Hashme, Chris Hesse, et al. Dota 2 with large scale deep reinforcement learning. *arXiv preprint arXiv:1912.06680*, 2019.
- [7] Ting Chen, Simon Kornblith, Mohammad Norouzi, and Geoffrey Hinton. A simple framework for contrastive learning of visual representations. In *International conference on machine learning*, pages 1597–1607. PMLR, 2020.
- [8] Xinlei Chen and Kaiming He. Exploring simple siamese representation learning. *arXiv preprint arXiv:2011.10566*, 2020.
- [9] Kurtland Chua, Roberto Calandra, Rowan McAllister, and Sergey Levine. Deep reinforcement learning in a handful of trials using probabilistic dynamics models. *arXiv preprint arXiv:1805.12114*, 2018.
- [10] Joery A de Vries, Ken S Voskuil, Thomas M Moerland, and Aske Plaat. Visualizing muzero models. *arXiv preprint arXiv:2102.12924*, 2021.
- [11] Marc Deisenroth and Carl E Rasmussen. Pilco: A model-based and data-efficient approach to policy search. In *Proceedings of the 28th International Conference on machine learning (ICML-11)*, pages 465–472. Citeseer, 2011.
- [12] Jean-Bastien Grill, Florian Strub, Florent Altché, Corentin Tallec, Pierre H Richemond, Elena Buchatskaya, Carl Doersch, Bernardo Avila Pires, Zhaohan Daniel Guo, Mohammad Gheshlaghi Azar, et al. Bootstrap your own latent: A new approach to self-supervised learning. *arXiv preprint arXiv:2006.07733*, 2020.
- [13] Danijar Hafner, Timothy Lillicrap, Jimmy Ba, and Mohammad Norouzi. Dream to control: Learning behaviors by latent imagination. *arXiv preprint arXiv:1912.01603*, 2019.
- [14] Danijar Hafner, Timothy Lillicrap, Ian Fischer, Ruben Villegas, David Ha, Honglak Lee, and James Davidson. Learning latent dynamics for planning from pixels. In *International Conference on Machine Learning*, pages 2555–2565. PMLR, 2019.
- [15] Danijar Hafner, Timothy Lillicrap, Mohammad Norouzi, and Jimmy Ba. Mastering atari with discrete world models. *arXiv preprint arXiv:2010.02193*, 2020.
- [16] Kaiming He, Haoqi Fan, Yuxin Wu, Saining Xie, and Ross Girshick. Momentum contrast for unsupervised visual representation learning. In *Proceedings of the IEEE/CVF Conference on Computer Vision and Pattern Recognition*, pages 9729–9738, 2020.

[17] Matteo Hessel, Joseph Modayil, Hado Van Hasselt, Tom Schaul, Georg Ostrovski, Will Dabney, Dan Horgan, Bilal Piot, Mohammad Azar, and David Silver. Rainbow: Combining improvements in deep reinforcement learning. In *Proceedings of the AAAI Conference on Artificial Intelligence*, volume 32, 2018.

[18] Thomas Hubert, Julian Schrittwieser, Ioannis Antonoglou, Mohammadamin Barekatain, Simon Schmitt, and David Silver. Learning and planning in complex action spaces. *arXiv preprint arXiv:2104.06303*, 2021.

[19] Lukasz Kaiser, Mohammad Babaeizadeh, Piotr Milos, Blazej Osinski, Roy H Campbell, Konrad Czechowski, Dumitru Erhan, Chelsea Finn, Piotr Kozakowski, Sergey Levine, et al. Model-based reinforcement learning for atari. *arXiv preprint arXiv:1903.00374*, 2019.

[20] Kacper Kielak. Do recent advancements in model-based deep reinforcement learning really improve data efficiency? *arXiv preprint arXiv:2003.10181*, 2020.

[21] Levente Kocsis and Csaba Szepesvári. Bandit based monte-carlo planning. In *European conference on machine learning*, pages 282–293. Springer, 2006.

[22] Ilya Kostrikov, Denis Yarats, and Rob Fergus. Image augmentation is all you need: Regularizing deep reinforcement learning from pixels. *arXiv preprint arXiv:2004.13649*, 2020.

[23] Anurag Koul. Pytorch implementation of muzero. <https://github.com/koulanurag/muzero-pytorch>, 2019.

[24] Michael Laskin, Kimin Lee, Adam Stooke, Lerrel Pinto, Pieter Abbeel, and Aravind Srinivas. Reinforcement learning with augmented data. *arXiv preprint arXiv:2004.14990*, 2020.

[25] Timothy P Lillicrap, Jonathan J Hunt, Alexander Pritzel, Nicolas Heess, Tom Erez, Yuval Tassa, David Silver, and Daan Wierstra. Continuous control with deep reinforcement learning. *arXiv preprint arXiv:1509.02971*, 2015.

[26] Volodymyr Mnih, Koray Kavukcuoglu, David Silver, Andrei A Rusu, Joel Veness, Marc G Bellemare, Alex Graves, Martin Riedmiller, Andreas K Fidjeland, Georg Ostrovski, et al. Human-level control through deep reinforcement learning. *nature*, 518(7540):529–533, 2015.

[27] Volodymyr Mnih, Adria Puigdomenech Badia, Mehdi Mirza, Alex Graves, Timothy Lillicrap, Tim Harley, David Silver, and Koray Kavukcuoglu. Asynchronous methods for deep reinforcement learning. In *International conference on machine learning*, pages 1928–1937. PMLR, 2016.

[28] Philipp Moritz, Robert Nishihara, Stephanie Wang, Alexey Tumanov, Richard Liaw, Eric Liang, Melih Elibol, Zongheng Yang, William Paul, Michael I Jordan, et al. Ray: A distributed framework for emerging {AI} applications. In *13th {USENIX} Symposium on Operating Systems Design and Implementation ({OSDI} 18)*, pages 561–577, 2018.

[29] Christopher D Rosin. Multi-armed bandits with episode context. *Annals of Mathematics and Artificial Intelligence*, 61(3):203–230, 2011.

[30] Tom Schaul, John Quan, Ioannis Antonoglou, and David Silver. Prioritized experience replay. *arXiv preprint arXiv:1511.05952*, 2015.

[31] Julian Schrittwieser, Ioannis Antonoglou, Thomas Hubert, Karen Simonyan, Laurent Sifre, Simon Schmitt, Arthur Guez, Edward Lockhart, Demis Hassabis, Thore Graepel, et al. Mastering atari, go, chess and shogi by planning with a learned model. *Nature*, 588(7839):604–609, 2020.

[32] Julian Schrittwieser, Thomas Hubert, Amol Mandhane, Mohammadamin Barekatain, Ioannis Antonoglou, and David Silver. Online and offline reinforcement learning by planning with a learned model. *arXiv preprint arXiv:2104.06294*, 2021.

[33] John Schulman, Sergey Levine, Pieter Abbeel, Michael Jordan, and Philipp Moritz. Trust region policy optimization. In *International conference on machine learning*, pages 1889–1897. PMLR, 2015.

[34] John Schulman, Philipp Moritz, Sergey Levine, Michael Jordan, and Pieter Abbeel. High-dimensional continuous control using generalized advantage estimation. *arXiv preprint arXiv:1506.02438*, 2015.

[35] John Schulman, Filip Wolski, Prafulla Dhariwal, Alec Radford, and Oleg Klimov. Proximal policy optimization algorithms. *arXiv preprint arXiv:1707.06347*, 2017.

[36] Max Schwarzer, Ankesh Anand, Rishab Goel, R Devon Hjelm, Aaron Courville, and Philip Bachman. Data-efficient reinforcement learning with self-predictive representations.

[37] David Silver, Aja Huang, Chris J Maddison, Arthur Guez, Laurent Sifre, George Van Den Driessche, Julian Schrittwieser, Ioannis Antonoglou, Veda Panneershelvam, Marc Lanctot, et al. Mastering the game of go with deep neural networks and tree search. *nature*, 529(7587):484–489, 2016.

[38] David Silver, Julian Schrittwieser, Karen Simonyan, Ioannis Antonoglou, Aja Huang, Arthur Guez, Thomas Hubert, Lucas Baker, Matthew Lai, Adrian Bolton, et al. Mastering the game of go without human knowledge. *nature*, 550(7676):354–359, 2017.

[39] Aravind Srinivas, Michael Laskin, and Pieter Abbeel. Curl: Contrastive unsupervised representations for reinforcement learning. *arXiv preprint arXiv:2004.04136*, 2020.

[40] Richard S Sutton and Andrew G Barto. *Reinforcement learning: An introduction*. MIT press, 2018.

[41] Yuval Tassa, Yotam Doron, Alistair Muldal, Tom Erez, Yazhe Li, Diego de Las Casas, David Budden, Abbas Abdolmaleki, Josh Merel, Andrew Lefrancq, et al. Deepmind control suite. *arXiv preprint arXiv:1801.00690*, 2018.

[42] Yuandong Tian, Jerry Ma, Qucheng Gong, Shubho Sengupta, Zhiyuan Chen, James Pinkerton, and Larry Zitnick. Elf opengo: An analysis and open reimplementation of alphazero. In *International Conference on Machine Learning*, pages 6244–6253. PMLR, 2019.

[43] Hado Van Hasselt, Arthur Guez, and David Silver. Deep reinforcement learning with double q-learning. In *Proceedings of the AAAI Conference on Artificial Intelligence*, volume 30, 2016.

[44] Hado van Hasselt, Matteo Hessel, and John Aslanides. When to use parametric models in reinforcement learning? *arXiv preprint arXiv:1906.05243*, 2019.

[45] Ziyu Wang, Tom Schaul, Matteo Hessel, Hado Hasselt, Marc Lanctot, and Nando Freitas. Dueling network architectures for deep reinforcement learning. In *International conference on machine learning*, pages 1995–2003. PMLR, 2016.

[46] Christopher John Cornish Hellaby Watkins. Learning from delayed rewards. 1989.

[47] Aurèle Hainaut Werner Duvaud. Muzero general: Open reimplementation of muzero. <https://github.com/werner-duvaud/muzero-general>, 2019.

[48] Denis Yarats, Amy Zhang, Ilya Kostrikov, Brandon Amos, Joelle Pineau, and Rob Fergus. Improving sample efficiency in model-free reinforcement learning from images. *arXiv preprint arXiv:1910.01741*, 2019.

A Appendix

A.1 Models and Hyper-parameters

As for the architecture of the networks, there are three parts in our model pipeline: the representation part, the dynamics part, and the prediction part. The architecture of the representation part is as follows:

- 1 convolution with stride 2 and 32 output planes, output resolution 48x48. (BN + ReLU)
- 1 residual block with 32 planes.

- 1 residual downsample block with stride 2 and 64 output planes, output resolution 24x24.
- 1 residual block with 64 planes.
- Average pooling with stride 2, output resolution 12x12. (BN + ReLU)
- 1 residual block with 64 planes.
- Average pooling with stride 2, output resolution 6x6. (BN + ReLU)
- 1 residual block with 64 planes.

, where the kernel size is 3×3 for all operations.

As for the dynamics network, we follow the architecture of MuZero [31] but reduce the residual blocks from 16 to 1. Furthermore, we add an extra residual link in the dynamics part to keep the information of historical hidden states during recurrent inference. The design of the dynamics network is listed here:

- Concatenate the input states and input actions into 65 planes.
- 1 convolution with stride 2 and 64 output planes. (BN)
- A residual link: add up the output and the input states. (ReLU)
- 1 residual block with 64 planes.

In the prediction part, we use two-layer MLPs with batch normalization to predict the reward, value, or policy. Considering the stability of the prediction part, we set the weights and bias of the last layer to zero in prediction networks. As for the reward prediction network, it predicts the sum of the rewards, namely value prefix: $r_t, h_{t+1} = \mathcal{R}(\hat{s}_{t+1}, h_t)$, where r_t is the predicted sum of rewards, h_0 is zero-initialized and hidden size of LSTM is 512. The architecture of the value prediction network is as follows:

- 1 1x1 convolution and 16 output planes. (BN + ReLU)
- Flatten.
- LSTM with 512 hidden size. (BN + ReLU)
- 1 fully connected layers and 32 output dimensions. (BN + ReLU)
- 1 fully connected layers and 601 output dimensions.

The horizontal length of the LSTM during training is limited to the unrolled steps $l_{\text{unroll}} = 5$, but it will be larger in MCTS as the dynamics process can go deeper. Therefore, we reset the hidden state of LSTM after $\zeta = 5$ steps of recurrent inference, where ζ is the valid horizontal length.

The design of the reward and policy prediction networks are the same except for the dimension of the outputs:

- 1 residual block with 64 planes.
- 1 1x1 convolution and 16 output planes. (BN + ReLU)
- Flatten.
- 1 fully connected layers and 32 output dimensions. (BN + ReLU)
- 1 fully connected layers and D output dimensions.

, where $D = 601$ in the reward prediction network and D is equal to the action space in the policy prediction network.

Here is the brief introduction of the training pipeline, taking one-step rollout as an example.

$$\begin{aligned}
 s_t &= \mathcal{H}(o_t) \\
 s_{t+1} &= \mathcal{H}(o_{t+1}) \\
 \hat{s}_{t+1} &= \mathcal{G}(s_t, a_t) \\
 v_t &= \mathcal{V}(s_t) \\
 p_t &= \mathcal{P}(s_t) \\
 r_t, h_{t+1} &= \mathcal{R}(\hat{s}_{t+1}, h_t) = \mathcal{R}(\mathcal{G}(s_t, a_t), h_t)
 \end{aligned} \tag{5}$$

, where \mathcal{H} is the representation network, \mathcal{G} is the dynamics network, \mathcal{V} is the value prediction network, \mathcal{P} is the policy prediction network, \mathcal{R} is the reward (*value prefix*) prediction network. o_t, s_t, a_t are observations, states and actions. h_t is the hidden states in recurrent neural networks.

Here is the training loss, taking one-step rollout as an example:

$$\begin{aligned}\mathcal{L}_{\text{similarity}}(s_{t+1}, \hat{s}_{t+1}) &= \mathcal{L}_2(sg(P_1(s_{t+1})), P_1(P_2(\hat{s}_{t+1}))) \\ \mathcal{L}_t(\theta) &= \mathcal{L}(u_t, r_t) + \lambda_1 \mathcal{L}(\pi_t, p_t) + \lambda_2 \mathcal{L}(z_t, v_t) \\ &\quad + \lambda_3 \mathcal{L}_{\text{similarity}}(s_{t+1}, \hat{s}_{t+1}) + c \|\theta\|^2 \\ \mathcal{L}(\theta) &= \frac{1}{l_{\text{unroll}}} \sum_{i=0}^{l_{\text{unroll}}-1} \mathcal{L}_{t+i}(\theta)\end{aligned}\quad (6)$$

, where \mathcal{L} is the total loss of the unrolled l_{unroll} steps, \mathcal{L}_1 is the Cross-Entropy loss, and \mathcal{L}_2 is the cosine similarity loss. Besides, P_1 is a 3-layer MLP while P_2 is a 2-layer MLP. The dimension of the hidden layers is 512 and the dimension of the output layers is 1024. We add batch normalization between every two layers in those MLP except the final layer. $sg(P_1)$ means stopping gradients.

We stack 4 historical frames, with an interval of 4 frames-skip. Thus the input effectively covers 16 frames of the game history. We stack the input images on the channel dimension, resulting in a $96 \times 96 \times 12$ tensor. We do not use any extra state normalization besides the batch norm and we choose reward clipping to keep better scales in the searching process.

Generally, compared with MuZero [31], we reduce the number of residual blocks and the number of planes as we find that there is no capability issue caused by much smaller networks in our EfficientZero with limited data. In another word, such a tiny network can acquire good performance in the limited setting.

Table 6: Hyper-parameters for EfficientZero on Atari games

Parameter	Setting
Observation down-sampling	96×96
Frames stacked	4
Frames skip	4
Reward clipping	True
Terminal on loss of life	True
Max frames per episode	108K
Discount factor	0.997^4
Minibatch size	256
Optimizer	SGD
Optimizer: learning rate	0.2
Optimizer: momentum	0.9
Optimizer: weight decay (c)	0.0001
Learning rate schedule	drop 2 times
Max gradient norm	10
Priority exponent (α)	0.6
Priority correction (β)	$0.4 \rightarrow 1$
Training steps	220K
Evaluation episodes	32
Min replay size for sampling	2000
Self-play network updating interval	200
Target network updating interval	400
Unroll steps (l_{unroll})	5
TD steps (k)	5
Policy loss coefficient (λ_1)	1
Value loss coefficient (λ_2)	0.25
Self-supervised consistency loss coefficient (λ_3)	2
LSTM horizontal length (ζ)	5
Dirichlet noise ratio (ξ)	0.3
Number of simulations in MCTS (N_{sim})	50
Reanalyzed ratio	0.99

For other details, we provide hyper-parameters in Table 6. It is notable that we train the model for 220k steps where we only collect data during the first 200k steps. In this way, the latter trajectories can be fully used in training. Besides, the learning rate will drop after every 100k training steps (from 0.2 to 0.02 and 0.002 at 100k, 200k steps respectively).

A.2 More Ablations

In the experiment section , we list some ablation studies to prove the effectiveness of each component. In this section, we will display more results for the ablation study.

Firstly, the detailed results of the ablation study of each component are listed in Table 7. In this table, We find that the full version of EfficientZero outperforms the others without any one of the components. Furthermore, for those environments EfficientZero can already solve, the performance is similar between the full version and the version without off-policy correction, such as Breakout, Pong, etc. In such a case, the off-policy issue is not severe, which is the reason for this phenomenon. Besides, for some environments with sparse rewards, the value prefix component matters, such as Pong; and for those with dense rewards, the state aliasing problem has less negative effects for the reward signals are sufficient, such as Qbert. As for the version without self-supervised consistency, the results of all the environments are much poorer.

Table 7: Ablations of the self-supervised consistency, end-to-end value prefix and model-based off-policy correction on more Atari games. (Scores on the Atari 100k benchmark)

Game	Full	w.o. consistency	w.o. value prefix	w.o. off-policy correction
Alien	1140.3	961.3	558	619.4
Amidar	101.9	32.2	31.0	256.3
Assault	1407.3	572.9	955.0	1190.4
Asterix	16843.8	2065.6	7330.0	13525.0
Bank Heist	361.9	165.6	273.0	297.5
BattleZone	17938.0	14063.0	9900.0	16125.0
Boxing	44.1	6.1	60.2	30.5
Breakout	406.5	237.4	379.2	400.3
ChopperCommand	1794.0	1138.0	1280	1487.5
Crazy Climber	80125.3	75550.0	106090.0	70681.0
Demon Attack	13298.0	5973.8	6818.5	8640.6
Freeway	21.8	21.8	21.8	21.8
Frostbite	313.8	248.8	235.2	227.5
Gopher	3518.5	1155	2792.0	2275.0
Hero	8530.1	5824.4	3167.5	9053.0
Jamesbond	459.4	154.7	380.0	356.3
Kangaroo	962.0	375.0	200.0	687.5
Krull	6047.0	4178.625	4527.6	3635.6
Kung Fu Master	31112.5	19312.5	25980.0	25025.0
Ms Pacman	1387.0	1090.0	1475.0	1297.2
Pong	20.6	-1.5	16.8	19.5
Private Eye	100.0	100.0	100.0	100.0
Qbert	15458.1	5340.7	6360.0	13637.5
Road Runner	18512.5	2700.0	3010.0	9856.0
Seaquest	1020.5	460.0	468.0	843.8
Up N Down	16095.7	3040.0	7656.0	4897.2
Normed Mean	1.904	0.881	1.482	1.475
Normed Median	1.160	0.340	0.552	0.836

In addition, we do the ablation study for the data augmentation technique in the consistency component to examine the effect of data augmentations. Here we choose several Atari games and train the model for 100k steps. The results are shown in Table 8. We can find that the version without data augmentation has similar performances while the version without consistency component is worse. This indicates that the improvement of the consistency component is basically from the self-supervised learning loss rather than the data augmentation.

Finally, we also do the ablation study for the MCTS root value and the dynamic horizon in the off-policy correction component. Here we choose several Atari games and train the model for 100k steps. As shown in Table 9, the version without dynamic horizon has poorer results than that without the MCTS root value. In the off-policy correction component, the dynamic horizon seems more important.

Table 8: Ablations of the data augmentation technique in the consistency component. Results show that the data augmentation has limited improvement in EfficientZero and the self-supervised training loss is more significant.

Game	Full	w.o. consistency	w.o. data augmentation
Asterix	6218.8	1350.0	1384.0
Breakout	388.8	12.0	365.2
Demon Attack	10536.6	5973.8	8730.0
Gopher	2828.8	1155.0	1823.75
Pong	19.8	-8.5	13.9
Qbert	15268.8	2304.7	14286.0
Seaquest	1321.0	460.0	1125.0
Up N Down	10238.1	3040.0	16380.0

Table 9: Ablations of the techniques (the MCTS root value and the dynamic horizon) in the off-policy correction component. The dynamic horizon seems more important than the MCTS root value when data is limited.

Game	Full	w.o. off-policy correction	w.o. dynamic horizon	w.o. MCTS root value
Asterix	6218.8	2706.3	3263.0	6288.0
Breakout	388.8	468.6	427.0	387.8
Demon Attack	10536.6	8640.6	9211.1	10063.0
Gopher	2828.8	2275.0	2459.2	2651.0
Pong	19.8	19.5	19.2	14.5
Qbert	15268.8	3948.4	7945	14738.0
Seaquest	1321.0	1248.0	1292.0	876.0
Up N Down	10238.1	3240.0	4772.0	9925.6

A.3 MCTS Details

Our policy searching approach is based on Monte-Carlo tree search (MCTS). We follow the procedure in MuZero [31], which includes three stages and repeats the searching process for $N_{\text{sim}} = 50$ simulations. Here are some brief introductions for each stage.

Selection In the selection part, it targets at choosing an appropriate unvisited node while balancing exploration and exploitation with UCT:

$$a^k = \left\{ \arg \max_a Q(s, a) + P(s, a) \frac{\sqrt{\sum_b N(s, b)}}{1 + N(s, a)} \left(c_1 + \log \left(\frac{\sum_b N(s, b) + c_2 + 1}{c_2} \right) \right) \right\} \quad (7)$$

, where $Q(s, a)$ is the average Q values after simulations, $N(s, a)$ is the total visit counts at state s by selecting action a , and $P(s, a)$ is the policy prior set in the expansion process. In each simulation, the MCTS starts from the root node s^0 . And for each time-step $k = 1 \dots l$ of the simulation, the algorithm will select the action a^k according to the UCT. Usually, $c_1 = 1.25$ and $c_2 = 19652$ according to the literature [37, 38, 15].

However, the default Q value of the unvisited node is set to 0, which indicates the worst state. To give a better Q-value estimation of the unvisited nodes, we evaluate a mean Q value mechanism in each simulation for tree nodes, similar to the implementation of Elf OpenGo [42].

$$\begin{aligned} \hat{Q}(s^{\text{root}}) &= 0 \\ \hat{Q}(s) &= \frac{\hat{Q}(s^{\text{parent}}) + \sum_b \mathbf{1}_{N(s, b) > 0} Q(s, b)}{1 + \sum_b \mathbf{1}_{N(s, b) > 0}} \\ Q(s, a) &:= \begin{cases} Q(s, a) & N(s, a) > 0 \\ \hat{Q}(s) & N(s, a) = 0 \end{cases} \end{aligned} \quad (8)$$

, where $\hat{Q}(s)$ is the estimated Q value for unvisited nodes to make better selections considering exploration and exploitation. s^{root} is the state of the root node and s^{parent} is the state of the parent node of s . In experiments, we find that the mean Q value mechanism gives a better exploration than the default one.

Expansion Then the newly selected node will be expanded with the predicted reward and policy as its prior. Furthermore, when the root node is to expand, we apply the Dirichlet noise to the policy prior during the self-play stage and the reanalyzing stage to give more explorations.

$$P(s, a) := (1 - \rho)P(s, a) + \rho\mathcal{N}_D(\xi) \quad (9)$$

, where $\mathcal{N}_D(\xi)$ is the Dirichlet noise distribution, ρ, ξ is set to 0.25 and 0.3 respectively. However, we do not use any noise and set ρ to 0 instead for those non-root node or during evaluations.

Backup After selecting and expanding a new node, we need to backup along the current searching trajectory to update the $Q(s, a)$. Considering the scales of values in distinct environments, we compute a normalized Q-value by using the minimum-maximum values calculated along with all visited tree nodes, which is applied in MuZero[31]. However, when the data is limited, the small difference between the minimum and maximum values will result in overconfidence in UCT calculation. For example, when all the Q-values in those visited tree nodes are in a range of 0 to 10^{-4} , the normalized Q-value of 10^{-5} and 5×10^{-5} will make a huge difference as one is normalized to 0.1 and another is 0.5. Therefore, we set a threshold here to reduce overconfidence in such occasions, which is called the soft minimum-maximum updates:

$$\bar{Q}(s^{k-1}, a^k) = \frac{Q(s^{k-1}, a^k) - \min_{(s,a) \in \text{Tree}} Q(s, a)}{\max_{(s,a) \in \text{Tree}} Q(s, a) - \min_{(s,a) \in \text{Tree}} Q(s, a) + \epsilon} \quad (10)$$

, where ϵ , the threshold to give a smooth range of the min-max bound, is set to 0.01.

After all the expansions in the MCTS, we will obtain average value and visit count distributions of the root node. Here, the root value can be applied in off-policy correction and the visit count distribution is the target policy distribution:

$$\pi(s, a) = \frac{N(s, a)^{1/T}}{\sum_b N(s, b)^{1/T}} \quad (11)$$

We decay the temperature of the MCTS output policy distribution here twice during training, at 50% and 75% of the training progress to 0.5 and 0.25 respectively.

A.4 Training Details

In this subsection, we will introduce more training details.

Pipeline As for the code implementation of EfficientZero, we design a paralleled architecture with a double buffering mechanism in Pytorch and Ray, as shown in Figure 6.

Intuitively, we will describe the training process in a synchronized way. Firstly, the data workers called self-play actors are aimed at doing self-play with the given model updated within 600 training steps and then they will send the rolled-out trajectories into the replay buffer. Then the CPU rollout workers attempt to prepare the contexts of those batch transitions sampled from the replay buffer, in which way only CPU resources are required. Afterward, the GPU batch workers reanalyze those past data with the given contexts by the given target model, and most of the time-consuming parts in this procedure are in GPUs. Considering the frequent utilization of CPUs and GPUs in MCTS, the searching process is assigned for those GPU workers. Finally, the learner will obtain the reanalyzed batch and begin to train the agent.

The learner, all the data workers, CPU workers, and GPU workers start in parallel. The data workers and CPU workers share the replay buffer to sample data while the CPU and GPU workers share a context queue for reanalyzing data. Besides, the learner and the GPU workers use a batch queue to communicate. In such a design, we can utilize the CPU and GPU as much as possible.

Self-play During self-play, the priorities of the transition to collect are set to the max of the whole priorities in replay buffer. We also update the priority in EfficientZero according to MuZero [31]: $P(i) = \frac{p_i^\alpha}{\sum_k p_k^\alpha}$, where p_i is the L1 error of the value during training. And the we scale with important sampling ratio $w_i = (\frac{1}{N \times P(i)})^\beta$. We set α to 0.6 and anneal β from 0.4 to 1.0, following prioritized replay [30]. However, we find the priority mechanism only improves a little with limited data. Considering the long horizons in atari games, we collect the intermediate sequences of 100 moves.

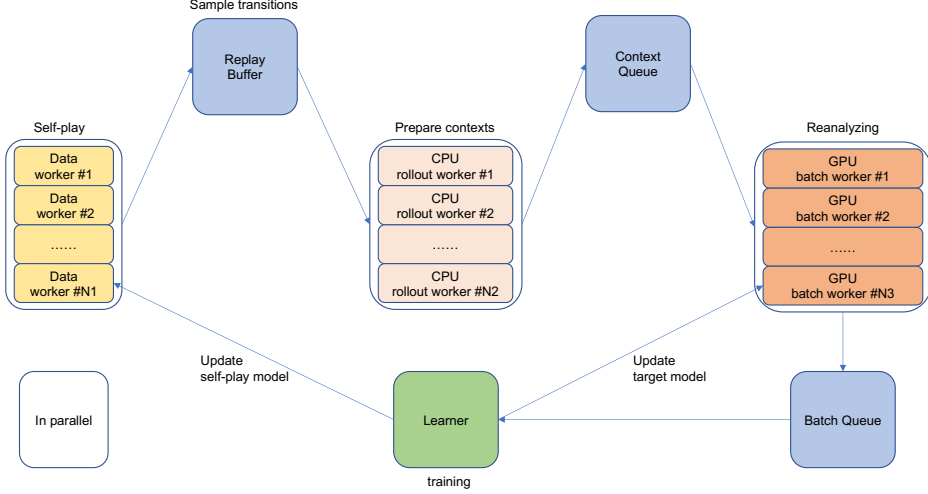


Figure 6: Pipeline of the EfficientZero implementation.

Reanalyze The reanalyzed part is introduced in MuZero [31], which revisits the past trajectories and re-executes the data with lastest target model to obtain a fresher value and policy with model inference as well as MCTS.

For the off-policy correction, the target values are reanalyzed as follows:

$$z_t = \sum_{i=0}^{l-1} \gamma^i u_{t+i} + \gamma^l \nu_{t+l}^{\text{MCTS}}, \quad (12)$$

$$l = (k - \lfloor \frac{T_{\text{current}} - T_{s_t}}{\tau T_{\text{total}}} \rfloor) \cdot \text{clip}(1, k), \quad l \in [1, k]$$

, where k is the TD steps here, and is set to 5; T_{current} is the current training steps, T_{s_t} is the training steps of collecting the data s_t , T_{total} is the total training steps (200k), and τ is a coefficient which is set to 0.3. Intuitively, l is to define how fresh the collected data s_t is. When the trajectory is stale, we need to unroll less to estimate the target values for the sake of the gaps between current model predictions and the stale trajectory rollouts. Besides, we replace the predicted value v_{t+k} with the averaged root value from MCTS ν_{t+l}^{MCTS} to alleviate the off-policy bias.

Notably, we re-sample Dirichlet noise into the MCTS procedure in reanalyzed part to improve the sample efficiency with a more diverse searching process. Besides, we reanalyze the policy among 99% of the data and reanalyze the value among 100% data.

A.5 Evaluation

We evaluate the EfficientZero on Atari 100k benchmark with a total of 26 games. Here are the evaluation curves during training, as shown in Figure 7.

A.6 Open Source EfficientZero Implementation

MCTS-based RL algorithms present a promising future research direction: to achieve strong performance with model-based methods. However, two major practical obstacles prevent them from being widely used currently. First, there are no high-quality open-source implementations of these algorithms. Existing implementations [47, 23] can only deal with simple state-based environments, such as CartPole [4]. Accurately scaling to complex image input environments requires non-trivial engineering efforts. Second, MCTS RL algorithms such as MuZero [31] require a large number of computations. For example, MuZero needs 64 TPUs to train 12 hours for one agent on Atari games. The high computational costs pose problems both for the future development of such methods as well as practical applications.

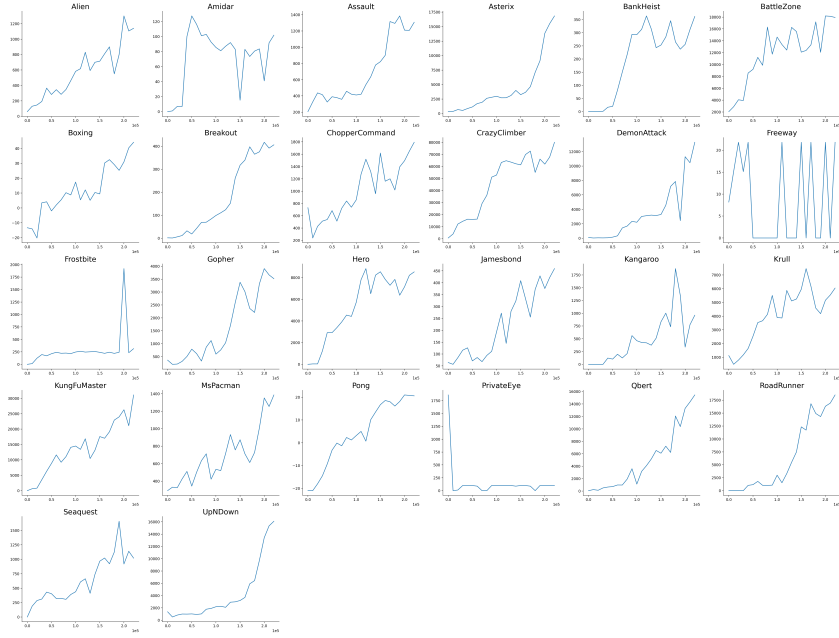


Figure 7: **Evaluation curves of EfficientZero on Atari 100k benchmark for individual games.** The average of the total rewards among 32 evaluation seeds is show on the y-axis and the number of total training steps is 220,000, shown on the x-axis.

We think our open-source implementation of EfficientZero can drastically accelerate the research in MCTS RL algorithms. Our implementation is computationally friendly. To train an Atari agent for 100k steps, it only needs 4 GPUs to train 7 hours. Our framework could potentially have a large impact on many real-world applications, such as robotics since it requires significantly fewer samples.

Our open-source framework aims to provide an easy way to understand the implementation while keeping relatively high compute efficiency. As shown in Fig. 8, the system is composed of four components: the replay buffer, the experience sampling actor, the reanalyze training target preparation module, and the training component.

To make sure the framework is easy to use, we implement them based on Ray [28], and the four components are implemented as ray actors which run in parallel. The main computation bottleneck is in the reanalyze module, which samples from the replay, and runs an MCTS search on each observation. To accelerate the reanalyze module, we split the reanalyze computation into the CPU part and the GPU part, such that computation on CPU and GPU are run in parallel. We use a different number of actors between CPU and GPU to match their total throughput. To increase the throughput on GPU, we also collocate multiple batch computation threads on one GPU, as in Tian et al. [42]. We also implement the MCTS in C++ to avoid performance issues with Python on large amounts of atomic computations.

We implement the MCTS by a couple of important techniques, which are quite crucial to improve the efficiency of the MCTS process. On the one hand, we implement batch MCTS to allow the agent to search a batch of trees in parallel, to enlarge the throughput of MCTS during self-play and reanalyzing targets. On the other, we choose C++ in the MCTS process. However, the process of

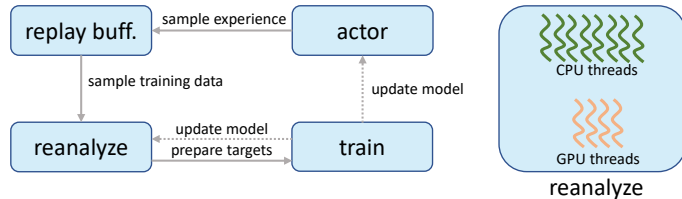


Figure 8: EfficientZero implementation overview.

MCTS needs to do searching as well as model inference, which needs to communicate with Pytorch. Therefore, we use Python to do model inference, C++ to do other atomic computations, and Cython to communicate between Python contexts and C++ contexts. In another word, we use pure C++ to do selection, expansion, and backup while using neural networks in Python. Meanwhile, we build a database to store the hidden states in Python while storing the corresponding data index during the searching process in C++. For more details of the implementation, please refer to <https://github.com/YeWR/EfficientZero>.